

RECENT RESEARCH INTO SOME AERODYNAMIC DESIGN
PROBLEMS OF SUBSONIC TRANSPORT AIRCRAFT

by

A. B. Haines
Aircraft Research Association Limited
Bedford, U.K.

**The Sixth Congress
of the
International Council of the
Aeronautical Sciences**

DEUTSCHES MUSEUM, MÜNCHEN, GERMANY/SEPTEMBER 9-13, 1968

Preis: DM 2.00

RECENT RESEARCH INTO SOME AERODYNAMIC DESIGN
PROBLEMS OF SUBSONIC TRANSPORT AIRCRAFT

A. D. BAINE

Research Director, Aerodynamics Division

British Aircraft Corporation

The Sixth Congress

of the

International Council of the

Aeronautical Sciences

DEUTSCHES MUSEUM, MUNICH, GERMANY, SEPTEMBER 9-13, 1968

RECENT RESEARCH INTO SOME AERODYNAMIC DESIGN PROBLEMS OF
SUBSONIC TRANSPORT AIRCRAFT

A.B. Haines
Chief Aerodynamicist, Aircraft Research Association Limited
Bedford, England

Abstract

The aims and results of recent research principally at A.R.A. into some design problems of subsonic transports are described. The emphasis is on how to obtain low drag in cruising flight and satisfactory buffet-free performance over the full flight envelope. In particular, the paper discusses how to design a three-dimensional wing to exploit recent advances in two-dimensional section design and how to devise satisfactory nacelle installations. The paper stresses the continuing need for research on the tunnel test techniques required to simulate flight behaviour, and to establish the exchange rates involved in design compromises between aerodynamic and other requirements.

1. Introduction

Over the past few years, a considerable amount of aerodynamic research relevant to subsonic transport aircraft has been undertaken at the Aircraft Research Association (A.R.A.) in Bedford. The research has been concentrated in areas where it is possible to use the A.R.A. experimental facilities, notably the 9ft x 8ft perforated-wall transonic tunnel supplemented by an 18inch x 8inch intermittent pressurized tunnel which is now producing two-dimensional aerofoil data at a Reynolds number of about $R = 7 \times 10^6$. The main emphasis therefore is on the drag in the cruise condition and on the study of the off-design performance, stability and control characteristics over the complete flight envelope from a Mach number of say, $M = 0.4$ upwards. There is no strictly low-speed tunnel at A.R.A. and so take-off and landing problems are not studied directly.

Wind-tunnel research to help the designer of a subsonic transport can be broadly classified under four headings, viz,

- (1) Fundamental research, e.g. to improve the methods for calculating the pressure distributions and boundary layer characteristics over wings and bodies in isolation and in combination. In other words, research to improve the methods and tools available to the designer,
- (2) Research to understand the performance of specific aircraft designs, to highlight their problem areas and so, to enable the designer to build more intelligently on past experience,
- (3) Closely allied to (2), research to help the designer interpret an aircraft specification in terms of suitable wing pressure distributions, isobar patterns, nacelle installations etc. The distinction between (1) and (3) therefore is that (3)

is research to establish desirable targets for the designer while (1) is research to help the designer to achieve these targets,

- (4) Research to improve testing techniques so that the full-scale flight behaviour can be predicted successfully from tunnel results.

Most of the research at A.R.A. comes under headings (2), (3) or (4). The paper describes some of the ways in which recent research is likely to contribute to the design of improved three-dimensional sweptback wing-body combinations and underwing or aft-fuselage nacelle installations. Increasing emphasis is now being placed on aimed research of type (3) but several of the illustrations in this paper have been taken from an analysis of data for various specific layouts, i.e. work of type (2). It should be stressed that the work at A.R.A. forms part of a national effort embracing other establishments and industry.

2. Wing Design

2.1 The High-speed Design Aims

In the past, one of the most powerful selling-points for a new subsonic transport has often been an increase in cruising speed and hence, a reduction in block time as compared with its predecessors. This may still be true in the future but only to a reduced extent. Rather, the emphasis will be on designing the most economic aircraft to meet a given specification. This will entail finding the best possible compromise between the aerodynamic, structural and engineering requirements. The change in emphasis also means that the best "high-speed" aerodynamic wing design is itself a compromise between various objectives. The probable aims would be to obtain

- (a) the highest possible M_D , the Mach number for the onset of the rapid increase in wave drag at a given C_L , for a given thickness/chord ratio and sweepback. This may be better expressed by saying that the aim will often be to achieve a target value of M_D with the thickest possible wing, for the sake of lower structure weight, increased fuel capacity etc. and with a modest and not too extreme sweepback for the sake of better take-off, landing and off-design characteristics,
- (b) as low a drag as possible at $M = M_D$. To judge from a recent study¹ of the cruise drag of a number of subsonic transport aircraft, this particular objective should be given added prominence in the initial design stage,

- (c) also, the smallest possible initial rate of increase of C_D with M beyond $M = M_D$. This point is important since the best cruise performance is usually obtained at a Mach number possibly 0.02 - 0.03 in excess of M_D and there will always be a tendency on occasion to fly as close to the buffet boundary as possible,
- (d) a satisfactory $M_D - C_L$ boundary with probably little variation in M_D with C_L . This could be particularly important for a short-range aircraft for which there were no dominant M_{cruise} , $C_{Lcruise}$ conditions,
- (e) a satisfactory margin between the drag-rise and flow separation boundaries, both in terms of C_L and below M_{cruise} and in terms of M above M_D at cruise C_L ,
- (f) a progressive flow breakdown at the stall giving not only a satisfactory useable C_{LMAX} but also adequate buffet warning and acceptable pitching moment characteristics.

Any single wing design considered for a particular application is unlikely to be the optimum solution for each of the above objectives, the designer will have to decide on the best compromise but the research such as that described in this paper should help him in making a satisfactory choice.

2.2 Choice of Pressure Distributions and Isobar Pattern

It is probable that before starting on the detailed design of the wing to meet the objectives set out above, the aspect ratio, taper ratio, minimum acceptable thickness/chord ratio and maximum acceptable sweepback will have been defined at least approximately by other considerations. The first aim will then be to design the wing to achieve a sufficiently high M_D at the design (usually the cruise) C_L . The normal procedure starts by choosing an upper-surface pressure distribution and thickness form for the equivalent two-dimensional section. Obviously, there are many alternative options even at this stage and the thickness/chord ratio for example that will prove acceptable can depend greatly on what option is selected. This point can be illustrated quite simply by referring to the predictions in Ref.2 for the family of shapes defined in Ref.3. These sections are designed to give a roof-top upper-surface pressure distribution back to a position x_R followed by a linear pressure rise to the trailing edge, combined with a thickness distribution such that the maximum velocity due to thickness also occurs at x_R . The importance of x_R as a design variable can be seen from Fig.1. This shows that for a given M_D , extending the roof-top from $x_R = 0.3$ to $x_R = 0.6$ gives an increase of about 0.3 in C_L for a given thickness/chord ratio or alternatively, allows an increase of 0.04 - 0.05 in thickness/chord ratio for a given design C_L . These trends cannot be exploited too far since ultimately, the boundary layer may not be able to

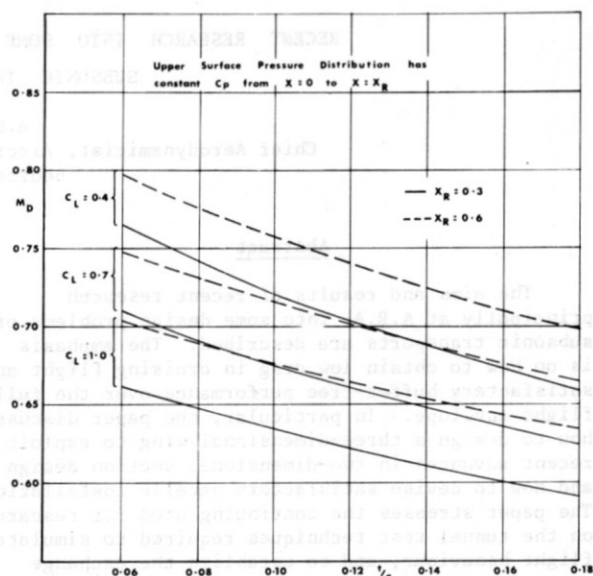


FIG.1 VARIATION OF DRAG RISE MACH NUMBER, M_D WITH DESIGN C_L , t/c AND ROOF TOP EXTENT

negotiate the adverse pressure gradient aft of the roof-top without separating even at full-scale Reynolds numbers. In some instances, this limit may be reached before $x_R = 0.6$. Leaving aside this particular issue, however, this class of section designs can still be rated as conservative; tests in the A.R.A. two-dimensional tunnel and elsewhere have shown that significantly higher values of M_D can be achieved for a given x_R , t/c and C_L , e.g. from extra loading at either the front or rear. Improvements could be obtained either by modifying the thickness form while still retaining the same upper surface pressure distribution or by modifying the latter. Fig.2, for example illustrates how two sections of the same thickness/chord ratio could be proposed to give the same predicted M_D at roughly the same C_L . The full-line curves in Fig.2 are for a section with $x_R = 0.5$, taken from the family just described. In this case, a shock-wave would be expected to form first at a position aft of the crest ($x_{CR} = 0.35$) at a Mach number close to the predicted M_D . The other section gives a pressure distribution of the peaky-type discussed in various papers^{4,5} by Pearcey and others. In this case, a local supersonic region terminated either by a shock or ideally, a largely isentropic recompression would form ahead of the crest at $M < M_D$; with increasing Mach number, the shock wave would move aft, passing over the crest, ($x_{CR} = 0.25$) at about $M = M_D$. The extra lift from the supersonic region ahead of the crest is one of the reasons why the total lift produced by the two sections is virtually the same. These two aerofoils are therefore equivalent in terms of M_D for a given t/c and C_L but even in two-dimensional flow, could well give a different C_D at M_D and a different off-design behaviour.

Other comparisons could be presented with for example, sections giving extra rear-loading but it would be wrong to suggest that the choice lies between different classes, e.g., roof-top or rear-loaded. The comparison in Fig.2 was included largely because it highlights how the choice of two-dimensional pressure distribution can have a

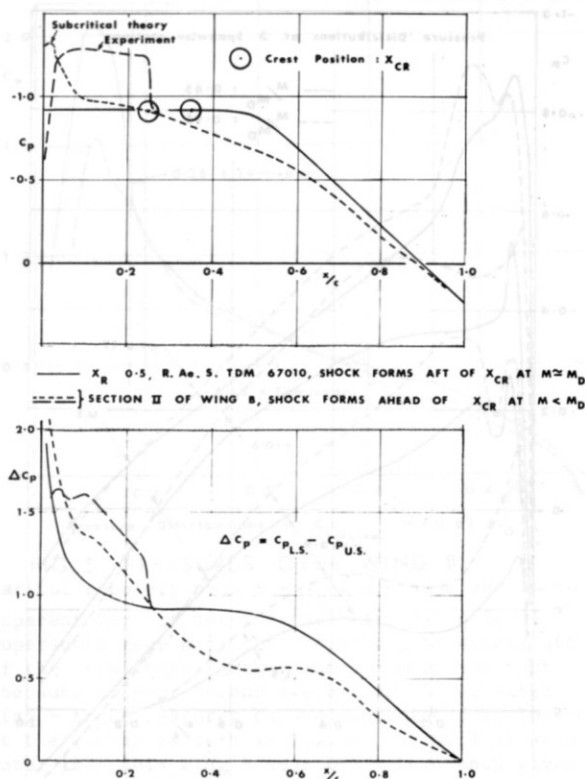


FIG. 2 COMPARISON OF TWO PRESSURE DISTRIBUTIONS GIVING SIMILAR C_L AT SAME M_D AND x/c

major effect on the problems encountered in designing the three-dimensional sweptback wing. It is fashionable - although not necessarily correct - to design the three-dimensional wing to obtain a "uniform isobar pattern" i.e. the same chordwise pressure distribution at all spanwise stations. For the roof-top type, this "merely" involves knowing how to vary the section shape across the span, how to shape the body and how to modify the planform near the tip, in order to counter the root- and tip-effects in subcritical flow. With a peaky-type distribution such as for section II in Fig.2, however, the flow at M_D is supersonic over part of the surface and therefore, retention of M_D as the design M for the three-dimensional wing implies that one can estimate how the three-dimensional root- and tip-effects are likely to affect this supercritical development. The alternative approach of designing for a lower Mach number where the flow would still be subcritical everywhere may also have its pitfalls since for a wing of say, 35° sweepback, this could mean reducing the design Mach number by as much as 0.15 - 0.2. These matters are currently being investigated in a research programme at A.R.A. but experimental results are not yet available.

Even when considering just the central part of the semi-span of a tapered wing, problems arise in deciding how best to allow for the variation in geometric sweepback from leading edge to trailing edge. Strictly, when dealing simply with the design point, one can argue⁶ in favour of thinking in terms of "equivalent 2-D and 3-D pressure distributions" rather than "equivalent sections". For example, to be equivalent to a roof-top distribution in 2-D flow, one needs to design for a "sloping roof-top" in 3-D flow, i.e., parallel to

the chordwise variation in C^* where C^* corresponds to $M = 1.0$ normal to the lines at constant x . To some extent, this must tend to reduce the advantages of a rearward extension of the "roof-top". The essential point to note is that at least when considering the first appearance of a shock wave, research over many years has supported the idea that it is the Mach-number distribution normal to the isobars that is significant, except possibly in regions where the isobar sweep is changing rapidly with position. There may therefore be a case for a spanwise variation not merely in the section shape but also in the target pressure distribution - in order to increase the isobar sweepback.

2.3 Effects of Choice on Drag at $M = M_D$

A recent assessment¹ of the measured drag in flight at cruise C_L for a number of subsonic transport aircraft has analysed the data in terms of a "figure-of-merit", E_{pr} defined as

$$E_{pr} = \frac{C_D - C_{D_{vi}}}{C_D}$$

where $C_{D_{vi}}$ = estimated vortex-induced drag coefficient at cruise C_L ,

and $C_{D_{pr}}$ = estimated profile drag coefficient at low speeds, obtained simply as the sum of the profile drag coefficients of the various component surfaces using form factors from the R.Ae.S. Data Sheets⁷ and assuming transition at the wing leading edge.

Computed on this basis, the values of E_{pr} for an idealised aircraft with no interference drag, no roughness drag, no drag due to excrescences etc. could be as low as 0.9 but in practice, even at low Mach number, it appears difficult to achieve values of less than about 1.25. Results for three of the aircraft, considered in Ref.1 are presented here in Fig.3. This shows the variation of E_{pr} with M/M_D as derived both from the flight data, and from model tests in the A.R.A. tunnel on the corresponding wing-fuselage configurations. In the case of the model data, the derived values of E_{pr} allow for the known transition positions. As would be expected, the values of E_{pr} for the model wing-fuselage are appreciably lower than for the aircraft in flight largely because one major source of interference drag, the nacelle installation, is missing and because various excrescences and other sources of "dirtiness drag" present on the aircraft are not simulated on the model. In all cases, there is an appreciable increase in E_{pr} with M below $M = M_D$ and it is significant that in each case, the tunnel data faithfully reflect the flight variation, thus suggesting that it is the wing-fuselage which is mainly responsible for this trend. This conclusion should not be accepted too literally because examples can be quoted where the nacelle installation drag at the cruise Mach number is higher than would be predicted on the basis of low speed data.

Analysis of the test data for the three examples has shown that the primary reason for the increase in E_{pr} by $M = M_D$ is different in each case:

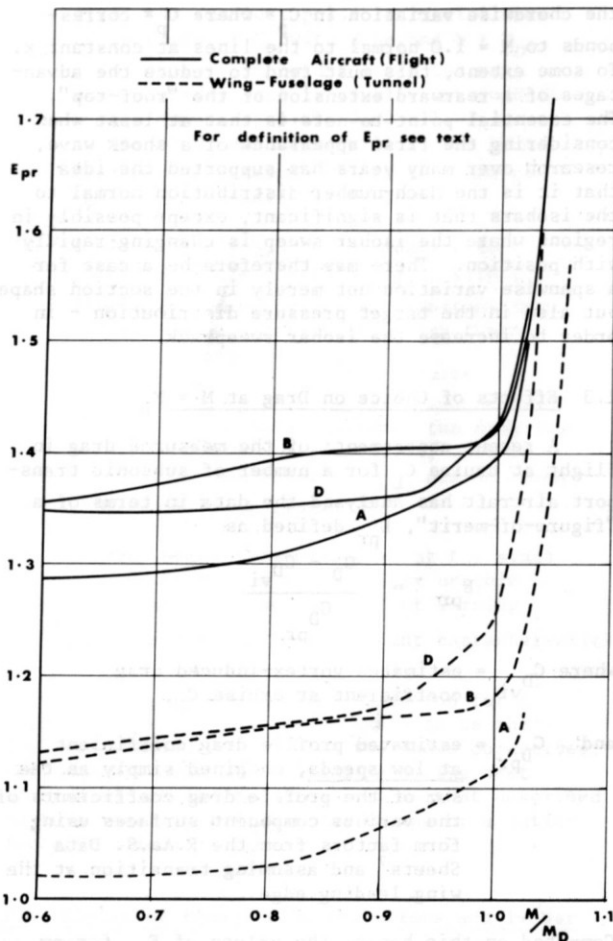


FIG. 3 VARIATION OF E_{pr} WITH M

an increase in subcritical wing profile drag (A), premature wave drag as a sectional effect somewhere along the span (B), or premature wave drag due to three-dimensional effects near the root (D).

For wing-body A, pressure measurements showed that the flow was subcritical everywhere up to at least $M = 0.95 M_D$; boundary layer traverses at the wing trailing edge indicated little change in profile drag coefficient with M near the wing root but a significant increase for the middle and outer parts of the span. There could be several reasons for these trends but the most likely explanation is to be found in the way the pressure distributions vary with M . Results for three stations are presented in Fig.4. Near the root, there is relatively little change with M at a constant C_L but further out, there is a pronounced increase with M in the adverse pressure gradient aft of about $0.3c$ at $\eta = 0.5$ or $0.15c$ at $\eta = 0.9$. Also, at the outer station and only at the outer station, there is a relatively high peak suction value near the leading edge on the lower surface, and the boundary layer has then to negotiate a steep adverse gradient back to about $0.2c$ and then, a further adverse gradient aft of about $0.4c$. It is worth noting that calculations by the method of Ref.9 did not fully predict the increases in profile drag actually observed in these measured results. This may indicate that an improved boundary-layer theory is needed to cope with

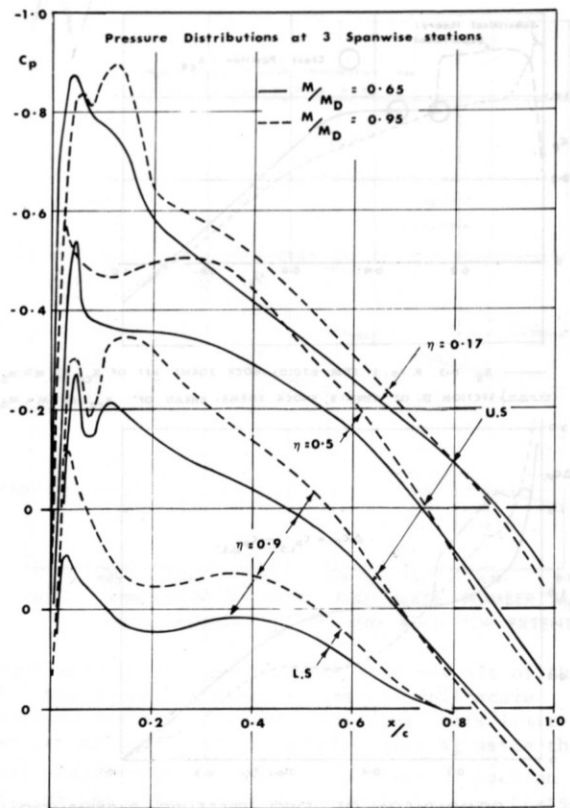


FIG.4 PRESSURES OVER WING A

pressure distributions of the present type, i.e. distributions where a steep adverse gradient is followed by a favourable gradient and then a further adverse gradient increasing in magnitude towards the trailing edge. Only then will it be possible to know how far one can go in this direction without incurring excess profile drag.

With wing-body B, some increase in E_{pr} with M has probably occurred even before $M = 0.6 M_D$ (Fig.3). The spanwise distribution of normal pressure drag, obtained by integrating measured pressure distributions showed that in this case, it is the region near $0.3 \times$ semispan that is mostly responsible. The reason for this can be seen from Fig.5 which compares the pressure stations at $\eta = 0.28$ and 0.18 at $M = 0.62 M_D$; to make the comparison clearer, the results are plotted against $\sqrt{x/c}$. At this Mach number, the pressures are still subcritical but at $\eta = 0.28$, the peak suction value (at $0.01c$) is very high and is followed by a particularly severe adverse gradient. To judge from the shape of the pressure distributions over the rear of the chord, there is an appreciable increase in boundary layer thickness aft of about $0.75c$ at $\eta = 0.23$; this would be consistent with a relatively high profile drag at this station. By $M = 0.7 M_D$, the velocities near the leading edge are already supersonic normal to the isobars and a normal shock, strong enough to induce a boundary-layer separation was observed near $M = 0.85 M_D$. Subsequently, the shock strength decreased until by $M = M_D$, there is merely an oblique shock followed by some isentropic recompression. These changes are therefore responsible for the characteristic shape of the $E_{pr} - M$ variation in this particular case (Fig.3); the

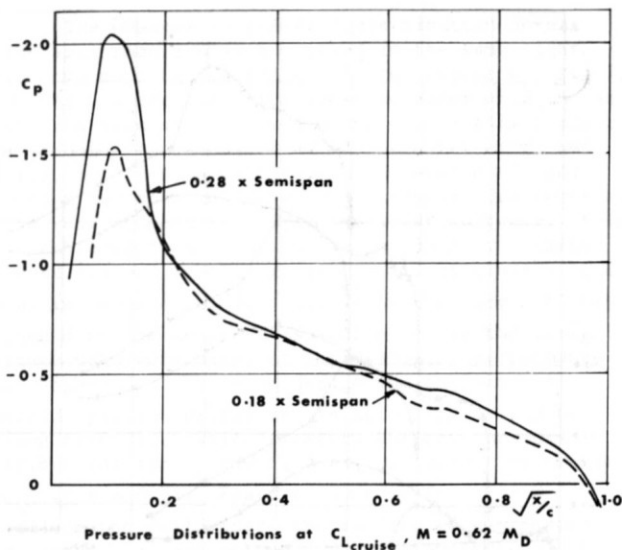


FIG. 5 PRESSURES OVER WING B

partial recovery near $M = M_D$ would have been more apparent were it not for the fact that a local supersonic region is then beginning to extend aft of the crest both further inboard near the root (because of poor isobar sweep) and on the outer wing - these features can be appreciated by looking at the isobar pattern in Fig.9a. It will be seen later that this wing B near 0.3 x semi-span gives a very favourable peaky-type development at higher Mach numbers but it should not be assumed from this one example that this can only be achieved at the expense of extra profile and/or wave drag at Mach numbers below design. Two-dimensional tests are pointing the way in this respect and one important aim of future research should be to develop the means whereby acceptable characteristics can be produced at all stations across the span of a three-dimensional wing without the need for too many experimental iterations.

Finally, the third example, wing-body D is a case where a premature increase in drag prior to $M = M_D$ can be traced to an increase in wave drag locally near the wing root. This can be seen from the results presented in Fig.6. In this case, there is a significant increase in the "drag creep" above about $M = 0.92 M_D$, i.e., a trend in the opposite sense to that observed with wing B. Pressure distributions were measured at two stations, one close to the body side and the other at 70% semispan. The results for the outer section showed that no shockwave was present until about $M = 0.97 M_D$ and that it passed over the crest at about $M = M_D$. Near the body-side, however, as can be seen from the lower graph in Fig.6, there is a notable change in the shape of the upper-surface pressure distribution above about $M = 0.91 M_D$ and this, therefore, correlates closely with the shape of the $C_D - M$ variation in the upper picture. Above $M = 0.91 M_D$, the local supersonic region starts extending rearward, e.g., to near 0.4c at $0.95 M_D$ and 0.5c at M_D . It must be emphasized however that this is far from being a poor wing-root design. To judge from the shape of the pressure distributions, the effective isobar sweepback near the rear of the supersonic region must be at least as great as the geometric sweepback; also, compared with many other designs, relatively high suction

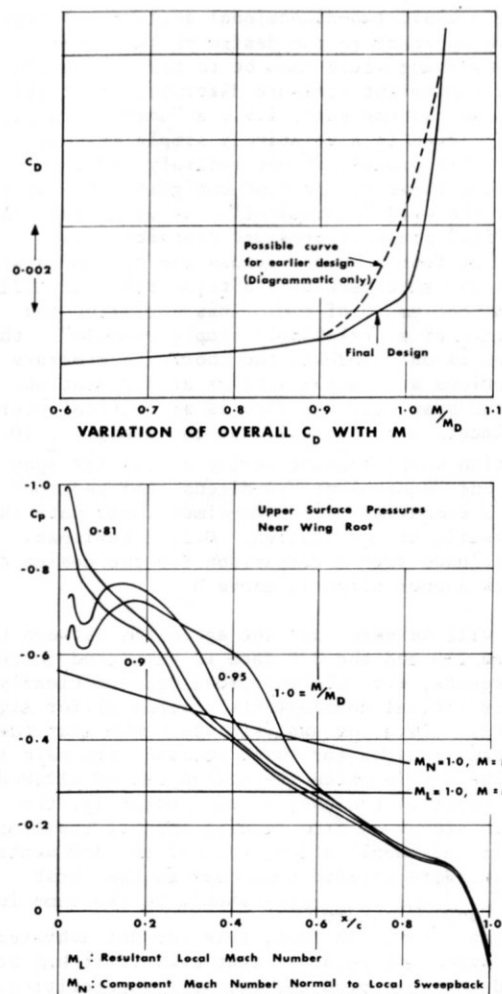


FIG. 6 ANALYSIS OF E_{pr} OR C_D VARIATION WITH M WING - BODY D

are still being maintained close to the leading edge at the root. It is relevant that while this design was being developed, modifications in the wing-root region gave material improvements in the actual value of M_D . Hence, it is possible to interpret the $C_D - M$ variation in Fig.6 by saying that the modifications were evidently successful in giving a substantial reduction in drag at Mach numbers near and just above the original M_D but not quite to the extent of reducing it to a level defined by an extrapolation of the subcritical creep. This point is illustrated diagrammatically in Fig.6.

It may seem from this discussion that some increase in E_{pr} at M_D is inevitable if only because of the need to compromise with other aerodynamic requirements. However, the real lesson is that the reasons for the standards achieved in respect of C_D at M_D can vary widely from one design to another: this conclusion is both a warning and a challenge to the designer to try and keep the sources of excess drag to a minimum.

2.4 Effects of Choice on Wing M_D and Off-design Supercritical Behaviour

Earlier, in section 2.2, comments were made about the various options open to the designer when

choosing a basic two-dimensional section. A conservative approach to the design of the three-dimensional wing would then be to try and obtain the same equivalent pressure distribution at all stations across the span, i.e., a "uniform isobar pattern". Even in a relatively simple example, however, this process is not entirely straightforward and there can be some ambiguity in what is meant by the word "equivalent". To illustrate this point, Fig.7 presents pressure distributions measured at four stations across the span of a wing of about 25° sweepback with a taper ratio of 0.33 and an aspect ratio of 8.0. This satisfies the description of a "relatively simple example" - the sweepback is only modest, the chordwise pressure distributions are fairly similar at all stations across the span, and the flow is subcritical everywhere almost up to M_D (0.73) at the design C_L (0.5). The section shape however varies across the span and as only one "equivalent two-dimensional section" was tested, a comparison with two-dimensional data is only possible at one station: 0.25 x semispan. Fig.7 includes such a comparison for the design C_L at a Mach number slightly above M_D .

It will be seen that the agreement between the converted 2-D and the 3-D data is very good in certain respects, e.g. the rear loading, but clearly, the supercritical developments already differ significantly. Detailed analysis has shown that there are several reasons for this; probably the main factor is the way in which the design method allowed for the taper of the wing or more strictly, the change in sweepback from leading edge to trailing edge. In this application, the 2-D and 3-D section geometries were related such that to the first order, C_{p3-D} and $C_{p2-D} \cos^2 \Lambda$ should be the same in subcritical flow. In fact, this was not achieved but the important point is that even if it had been, it would not have produced the same supercritical development. For example, let us suppose that the C_{p2-D} distribution were of a roof-top type. The C_{p3-D} distribution derived on the above basis would then have a peak at the rear of the roof-top as for the wing in Fig.7, but to give an equivalent flow development in the initial supercritical range, exactly the opposite is required. Strictly, to be equivalent to a roof-top in 2-D flow, the 3-D distribution should be a "sloping roof-top" parallel to the chordwise variation of M_N where M_N is defined as previously - see Fig.7. It follows that it may be preferable to think in terms of "equivalent pressure distributions" rather than "equivalent sections" but even then, the eventual supercritical development could still differ significantly since leaving aside other three-dimensional factors, it must still depend on both the pressure distribution and the surface curvature distribution.

It is clear from Fig.7 that the method used for converting from 2-D to 3-D has led to some reduction in M_D at the design C_L . For some applications, this could have been serious but in this case it did not conflict with the design aims which were to obtain a high useable C_L at all Mach numbers up to the cruise value, and a satisfactory flow breakdown across the wing at the stall. Other considerations such as the value of M_D at the cruise C_L were of less importance - always provided some minimum target figure was achieved.

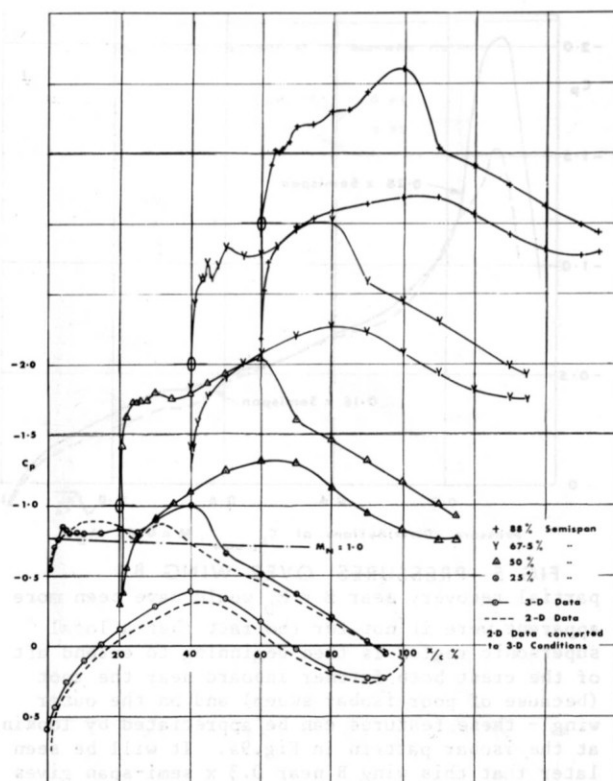


FIG. 7 PRESSURE DISTRIBUTION FOR 25° SWEEPBACK WING AT $C_{L_{DESIGN}}$; $M = 0.74 = (M_D + 0.01)$, $A = 8$, $\Lambda_o = 27.5^\circ$, $\Lambda_{1/4} = 15.5^\circ$

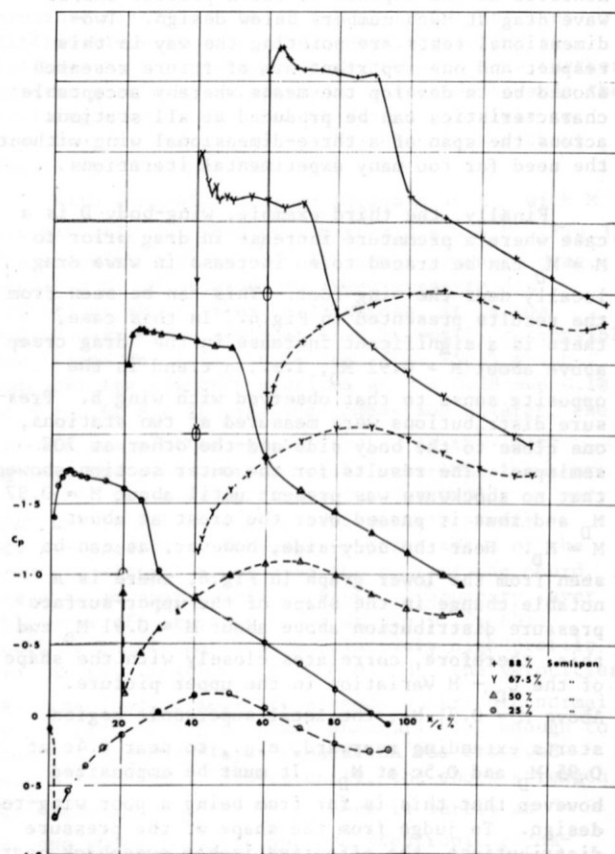


FIG. 8 PRESSURE DISTRIBUTION FOR 25° SWEEPBACK WING AT $C_L = C_{L_{DESIGN}} + 0.4$, $M = 0.7$

The changes in pressure distribution across the span should also be viewed in the same light. The two main trends evident at the cruise C_L , Fig.7, are (i), a decrease from inner to outer wing in the suction values near the leading edge - this leads to a stronger shock near 0.4c on the outer wing, and (ii), a reduction particularly between 0.675 and 0.88 x semispan in the adverse pressure gradients at the rear of both the upper and lower surfaces - this is achieved by a reduction in the local thickness/chord ratio. At the cruise C_L , (i) is clearly harmful in terms of M_D and (ii) is unnecessary but they should not be regarded as weaknesses in the design since both were aimed at improving the performance at higher C_L . The wing design was in fact outstandingly successful in its main aims as can be seen from Fig.8 which presents the pressure distributions for $C_L = 0.9$, i.e., 0.4 above the cruise C_L , at $M = 0.71$. Features to note from Fig.8 include the following: no trailing edge pressure divergence at any of the four stations; the shock front swept back at an angle greater than the local geometric sweepback; some isentropic recompression ahead of the shock at all four stations, and a fair degree of loading at the rear, again at all four stations.

The results for this wing have shown therefore that the idea of designing for essentially a roof-top pressure distribution over the upper surface at the cruise condition and shaping the leading edge to obtain some favourable peaky-type development at higher C_L is an attractive concept, particularly when good results are required over a wide range of operating C_L .

As a second example of supercritical flow development, the discussion for wing B in section 2.3 above can be continued to higher Mach numbers. Isobar patterns at the cruise C_L are presented in Fig.9a, b for $M = M_D$ and $M = M_D + 0.04$ respectively. The flow at $M = M_D$ has already been discussed. At station I, it appears that there is no normal shock but just an oblique shock and some isentropic recompression; conditions are in fact somewhat better than at lower Mach numbers. Further outboard, near station II, the main shock is near 0.2c and as can be seen by comparing Figs.9a, b, is moving rapidly aft with increasing Mach number. As a result, the sweepback of the shock front between stations I and II at $M = M_D + 0.04$ is considerably greater than the local geometric sweepback. One would expect therefore that the rate of increase with Mach number in the wave drag associated with this shock front would be less near I than near II (Fig.9b). At first sight, however, this is not borne out by the variation of the local section drag coefficients, ΔC_{D_L} , as derived from the measured pressure distributions. These are shown in Fig.9c, plotted in the form of ΔC_{D_L} vs. $(M - M_D)$ where ΔC_{D_L} is the increment in C_{D_L} compared with the value at $M = M_D$, and M_D is the drag-rise Mach number for the wing as a whole. The variation in the overall C_D is plotted below for comparison. It is clear that a spanwise integration of the values of $\frac{c}{c} \Delta C_{D_L}$ would yield a variation with Mach number broadly similar to that obtained in the overall measurements but the changes across the span in the ΔC_{D_L} variation are

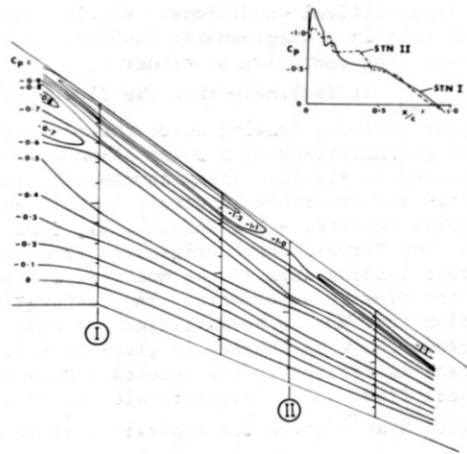


FIG. 9a ISOBARS ON WING B AT $C_{L_{DESIGN}}$, $M = M_D$

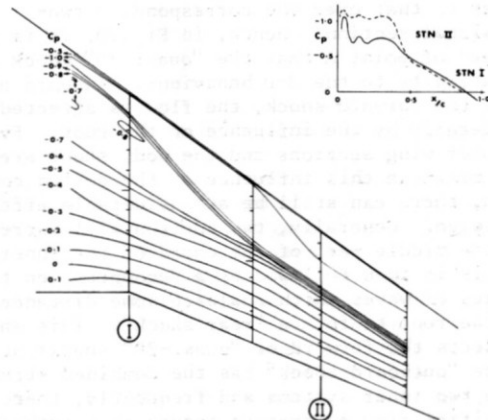


FIG. 9b ISOBARS ON WING B AT $C_{L_{DESIGN}}$, $M = M_D + 0.04$

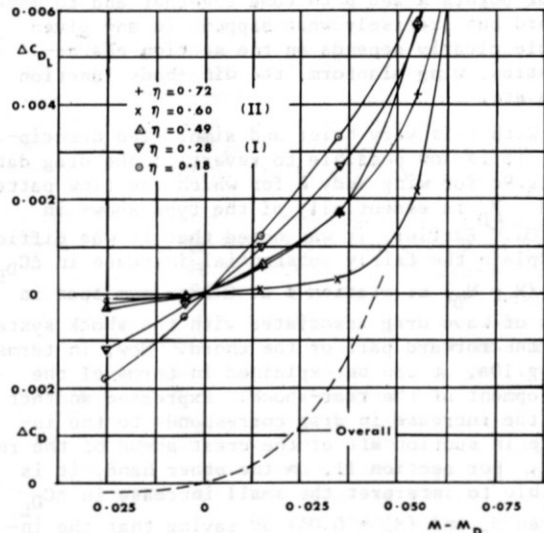


FIG. 9c VARIATION OF C_D WITH m BEYOND WING-BODY B

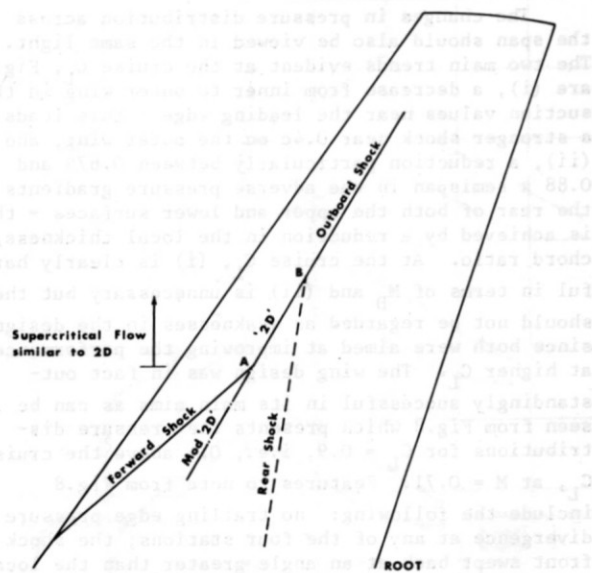
somewhat unexpected. Despite what was forecast above, it is section II which appears to give the most favourable results in the range up to $(M_D + 0.04)$.

To understand this apparent anomaly, one must consider how three-dimensional effects control the

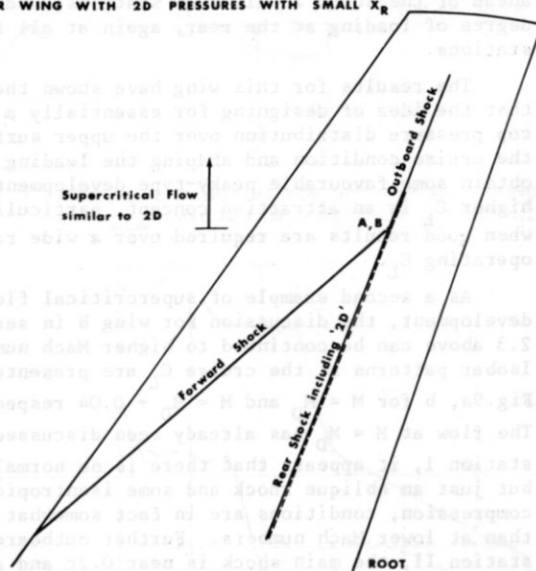
development of the flow over the sweptback wing under supercritical conditions. Fig.10 helps to explain this in a diagrammatic fashion. For any sweptback wing operating at either $C_L > C_{L_{design}}$ or $M > M_{design}$, it is likely that the flow over

the upper surface, leaving aside the tip region, will be characterised by a 3 (or 4)-shock system as illustrated in Fig.10. These shocks were first explained and described in detail by Hall and Rogers in several reports, e.g., Refs.10, 11, from the N.P.L. The forward shock originates from either the wing-root leading edge or the most forward point where the flow is supersonic. The mathematical condition that has to be satisfied for this shock to lie across the wing surface is given in Ref.11; its sweepback is related to the resultant Mach number of the local flow and so increases with C_L at a given M or with M at a given C_L ; typically, it is around 50° . The main significance of the forward shock is that it marks the inward boundary of the region in which the supercritical flow development can be similar to that over the corresponding two-dimensional section. Hence, in Fig.10, it is only outboard of point A that the "quasi-2D" shock bears some affinity to the 2-D behaviour. Inboard and aft of the forward shock, the flow is affected considerably by the influence of the root. Even if the inner wing sections and the body shape are such as to minimise this influence at the design condition, there can still be a considerable effect at off-design. Generally, the suction will increase over the middle part of the chord of the inner wing and this is then followed by a recompression through a series of waves which coalesce some distance out from the root to form a "rear shock". This shock intersects the forward or "quasi-2D" shocks at point B. The "outboard shock" has the combined strength of the two inner systems and frequently, therefore, the initial flow separation occurs just outboard of point B. As the Mach number is increased further beyond the design value, the general tendency will be for points A and B to come together and to move inboard but precisely what happens in any given example clearly depends on the section characteristics, wing planform, the wing-body junction shape etc.

With this very brief and simplified description, it is now possible to revert to the drag data in Fig.9c for wing-body B for which the flow pattern for $M > M_D$ is essentially of the type shown in Fig.10a. Earlier, it was noted that it was difficult to explain the fairly substantial increase in ΔC_{DL} with $(M - M_D)$ at station I at $0.28 x$ semispan in terms of wave drag associated with the shock system over the forward part of the chord. Now, in terms of Fig.10a, it can be explained in terms of the development of the rear-shock. Expressed another way, the increase in drag corresponds to the increase in suction aft of the crest ahead of the rear shock. For section II, on the other hand, it is possible to interpret the small increase in ΔC_{DL} between M_D and $(M_D + 0.04)$ by saying that the increase in wave drag has been partly offset by a reduction with Mach number in the root-influence on this section. This can be seen by comparing the pressure distributions for section 2 inset in Figs. 9a, b. The relatively high suction near $0.3 - 0.4c$ at $M = M_D$ were not observed in the tests on the equivalent two-dimensional section and can probably be ascribed to root-influence. No such



(a) FOR WING WITH 2D PRESSURES WITH SMALL X_R



(b) FOR WING WITH 2D PRESSURES WITH LARGE X_R

FIG. 10 TYPICAL SHOCK PATTERNS AT $M > M_{DESIGN}$ OR $C_L > C_{L_{DESIGN}}$

irregularities were observed aft of the main shock at $(M_D + 0.04)$ or in other words, this section then lies outboard of points A and B. ΔC_{DL} can therefore be a poor indication of the wave drag associated with the main shock front; the difficulty lies in knowing how C_{DL} would vary with Mach number in the absence of a shock wave. In the present case, the implication is that under such conditions, C_D would decrease with Mach number at station II.

Finally, the comparison between Figs.10a, b has been included in order to illustrate that the choice of basic design pressure distribution can have a major effect on the way the 3 (or 4)-shock system develops at off-design conditions. The two pictures correspond diagrammatically with the two alternative 2-D sections considered in Fig.2.

With small x_R , as in Fig.10a, the tendency is for the quasi-2D shock to link on the inner wing with the forward 3D-shock, thus leaving the rear-shock as a clearly defined separate front. With large x_R as in Fig.10b, the quasi-2D shock tends to link with the rear shock leaving the forward shock as the separate system. Obviously, these pictures and this description are grossly over-simplified but even so, certain conclusions are valid. For example, the proportion of the wing span over which the local supersonic region can develop as in two-dimensional flow is clearly greater in case (a); also, with (b), there is a greater likelihood that the supersonic region ahead of the rear shock develops in a manner completely uncontrolled by any expansion field being generated near the leading edge. It is not however the aim of this paper to pronounce in favour of (a) or (b). This would be both premature and unwise particularly as it is really misleading to think that there are just two classes of design. The distinctions have been deliberately overdrawn to simplify the discussion and to highlight the problems that are being investigated in current research.

2.5 Concluding Remarks on Wing-design Research

Examples have been given of how the choice of basic pressure distributions and isobar patterns can affect the subcritical drag, the drag-rise Mach number and the supercritical behaviour. It is clear that the best possible wing design for any given application is always likely to be a matter of compromise between different requirements. This is a decision for the designer; research can only help to provide the figures on which to base the compromise and the factors which should be taken into account. It is hoped that the examples have helped in these respects.

It is however worth noting three general conclusions:

- (1) When developing any new wing design, it is vital that detailed pressure distributions and if possible, boundary layer traverses at the trailing edge should be obtained at the earliest possible opportunity. Only in this way can one track down the sources of excess drag and the true reasons for any undesirable off-design performance,
- (2) In the past, there may have been too much stress on obtaining the best value of M_D with too little regard for C_D at M_D or for dC_D/dM near M_D ,
- (3) The choice of a suitable design pressure distribution cannot be assessed on two-dimensional evidence alone; three-dimensional effects can have a powerful influence particularly at supercritical speeds.

3. Scale Effects: Influence of Present Design Trends

No discussion of recent wing research would be complete without some reference to how present design trends, e.g. to thicker, more highly-loaded sections are affecting the chances of reproducing the true full-scale behaviour in model tests at moderate Reynolds numbers. This is now a problem even at subcritical speeds. Present trends are

increasing the likelihood of a boundary layer separation occurring towards the rear of both the upper and lower wing surfaces. Clearly, a design aim would be to avoid this happening at the cruise condition, full-scale but this may be difficult to ensure in the model tests. Also, even though a rear-separation may be present full-scale at higher C_L , off-design conditions, one still needs to know how to extrapolate the model data to obtain a reliable idea of the full-scale separation boundary.

Scale effects at high subsonic speeds have of course been studied for many years and a review¹² was published in 1954 giving advice on the methods that should be used for fixing boundary-layer transition in model tests. The main conclusion of this paper was that provided adequate steps were taken to ensure a turbulent boundary layer at the foot of the shock, test Reynolds numbers greater than about $R = 1.5 \times 10^6$ should be adequate. Most of the evidence then available however referred to thin sections operating at relatively low lift coefficients for which any shock-induced separation typically took the form of a bubble with the separation point at the foot of the shock and with the reattachment point progressively moving rearward with increases in Mach number or incidence. Under these conditions, major changes in the circulation round the wing section did not occur until the bubble had extended to the wing trailing edge and similarly, the divergence of the trailing-edge pressure was frequently used successfully as a guide to the onset of buffet. The incipient rear-separation tendency of many modern designs however opens up the possibility of a major interaction between the two forms of separation. Indeed, test data have shown that the existence of merely a weak shock with a pressure-rise which in itself would be insufficient to provoke a separation, can modify considerably the rear-separation characteristics - usually but not always in an adverse sense. It follows that unlike the flow model just described for thin sections, it is now possible for the separation point to move forward from near the trailing edge to near the foot of the shock as the Mach number is increased in the supercritical range. Under these conditions, scale effects must be expected up to much higher Reynolds numbers than the $R = 1.5 \times 10^6$ value quoted earlier.

A detailed account of these separation characteristics is given in Ref.13 but one figure is included here by way of illustration. Pressure distributions are presented in Fig.11 for a 55° sweptback wing design at low supersonic speeds. They are plotted as graphs of $M_N - x/c$ and in this form, they can also be taken to refer to say, a 35° sweptback wing at $M = 0.85$. The data for $R = 8 \times 10^6$ and 12×10^6 are from A.R.A. tests; those for $R = 2 \times 10^6$ from N.P.L. tests on a smaller model of the same design. At subsonic speeds, at the same incidence, a rear separation was only observed at $R = 2 \times 10^6$ and the results for $R = 8 \times 10^6$ and 12×10^6 were virtually identical. By $M = 1.1$, however, when a shock wave has formed near $0.45c$, some differences are evident between the data for even the two higher Reynolds numbers and by $M = 1.15$, these differences have become quite pronounced: a rear separation is now present at all the Reynolds numbers. It occurs aft of about $0.85c$ at $R = 12 \times 10^6$, $0.6c$ at $R = 8 \times 10^6$ and aft of the shock at $R = 2 \times 10^6$. The scale effect on the position and apparent strength of the

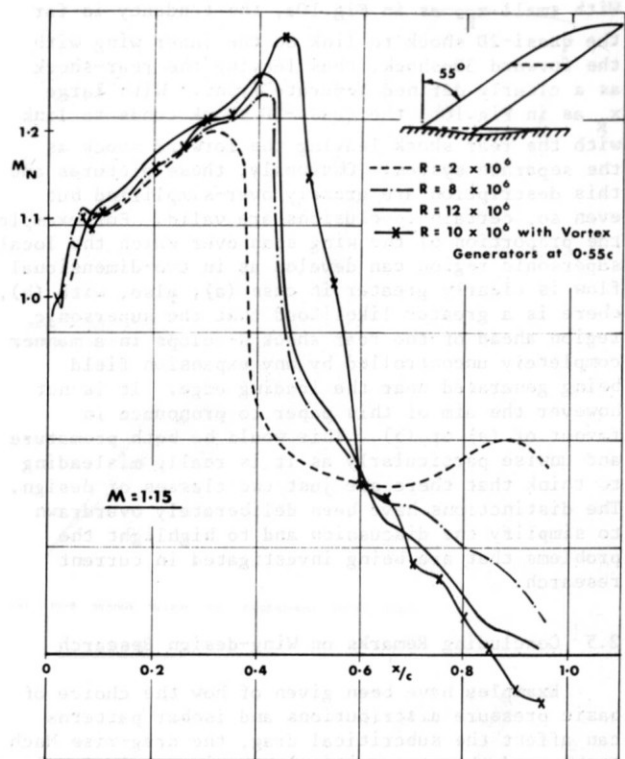
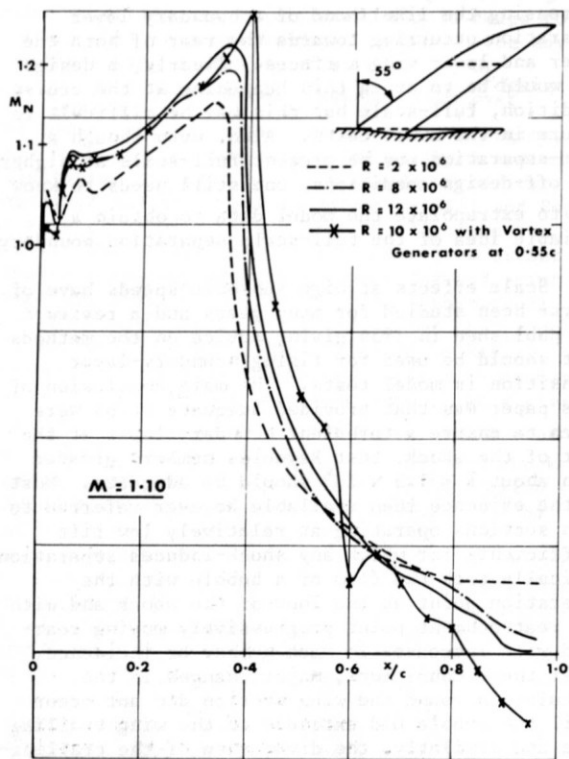


FIG. 11 REYNOLDS NUMBER EFFECTS FOR 55° SWEEP WING $\alpha = 4^\circ$

shock is however only marginal above $R = 8 \times 10^6$.

Results as striking as those in Fig. 11 prompt the question as to whether a change in the testing techniques could minimise scale effect of this nature. All the recent evidence confirms the earlier conclusion that one should ensure that the boundary layer is turbulent at the foot of the shock. This means that transition-free tests resulting in a laminar boundary layer at the shock are unacceptable. On the other hand, as regards a rear-separation, it is clearly important to try and represent as closely as possible, the full-scale boundary layer thickness at the shock. Hence, even though transition on the full-scale aircraft would be expected to occur near the leading edge, it may be permissible and indeed desirable, to allow transition to be further downstream in the model tests, always provided that it is ahead of the shock. It does not necessarily follow that the roughness band should be moved aft to say, 0.3c: the effects of the extra roughness height that would then be needed to fix transition would tend to offset the expected gain from the rearward movement of transition position. Hence, it may be preferable to retain a forward position for the roughness band but to reduce the size of the disturbance to the smallest that will trigger transition ahead of the shock. There are obvious disadvantages to this technique: for example, to interpret the drag data, one would need to establish the actual transition positions for the complete $M - C_L$ range of interest and this could be very laborious for a test on a three-dimensional wing; also, for the inner part of the wing, it may be important under certain conditions to ensure that the boundary layer is turbulent at the forward shock. For these reasons, it

seems that the correct practice for quite a wide class of designs, provided the test Reynolds number is at least $R = 3 \times 10^6$ (say), is that two tests should be made, viz,

- (i) a test with the minimum roughness band required to produce transition immediately downstream of the band. This is to obtain the drag at low C_L and is proposed on the assumption that even at the model Reynolds number, no rear-separation is present at the cruise C_L , and at Mach numbers up to just beyond $M = M_D$,
- (ii) a test with a smaller roughness band (or even natural transition if this gives a turbulent boundary layer at the most forward of the shock waves) to give the most reliable idea of the separation characteristics and hence, the off-design lift and pitching moment behaviour etc.

In any event, it is most important that the roughness band should not only be of minimum height but should be as narrow as possible and should be positioned downstream of any severe adverse pressure gradient near the leading edge, the overriding aim being to produce as thin a turbulent boundary layer as possible. Typically, in tests in the A.R.A. tunnel on models of 10" - 18" chord, the bands are about 0.004" high, 0.05" wide and are sited at positions varying from 0.05c to 0.15c, depending on the wing pressure distributions.

Another possible technique that has been used on several occasions is to add some vortex generators or other form of boundary-layer control

downstream of the shock but upstream of where the rear-separation tends to occur. This idea was tried on the 55° wing referred to above and Fig.11 shows the pressure distributions obtained with generators at 0.55c; the results with the generators alternatively at 0.75c were broadly similar. It will be seen that the addition of the generators has resulted in a notably better pressure recovery at the trailing edge and a somewhat more rearward shock position. These results may well be representative of the full-scale behaviour with generators fitted but they may be somewhat better than the full-scale behaviour without generators. This is because the vortices induced by the generators do more than merely thin the boundary layer. Even so, this could be a useful and valid technique. It would show what could be achieved as a separation boundary in flight. Whether vortex generators would be needed to achieve this boundary would be a matter for experiment on the full-scale aircraft. Clearly, the attractiveness of this approach depends on whether satisfactory results can be obtained at model scale with a small number of small generators giving only a minimal drag penalty under conditions of unseparated flow.

So far in this discussion, it has been suggested that any scale effects are in the sense that the results at low Reynolds number are necessarily worse than those at higher Reynolds numbers. It would be wrong however to accept this as a general conclusion; the process may well not be monotonic. Fig.12 for example considers an aerofoil from the family in Ref.3. In inviscid flow, this gives a roof-top pressure distribution back to about 0.6c on the upper surface at $C_L = 0.95$, $M = M_D = 0.65$. Calculations were then made using the method of Ref.14 to find the pressure distributions for the same C_L and section geometry at respectively $R = 30 \times 10^6$ and $R = 1 \times 10^6$. A reduction in Reynolds number implies a growth in the boundary layer displacement thickness, more on the upper surface than on the lower surface and hence, a change in the effective camber-line and a reduction in the rear-loading. As a result, to maintain the same C_L , the incidence has to be increased. The

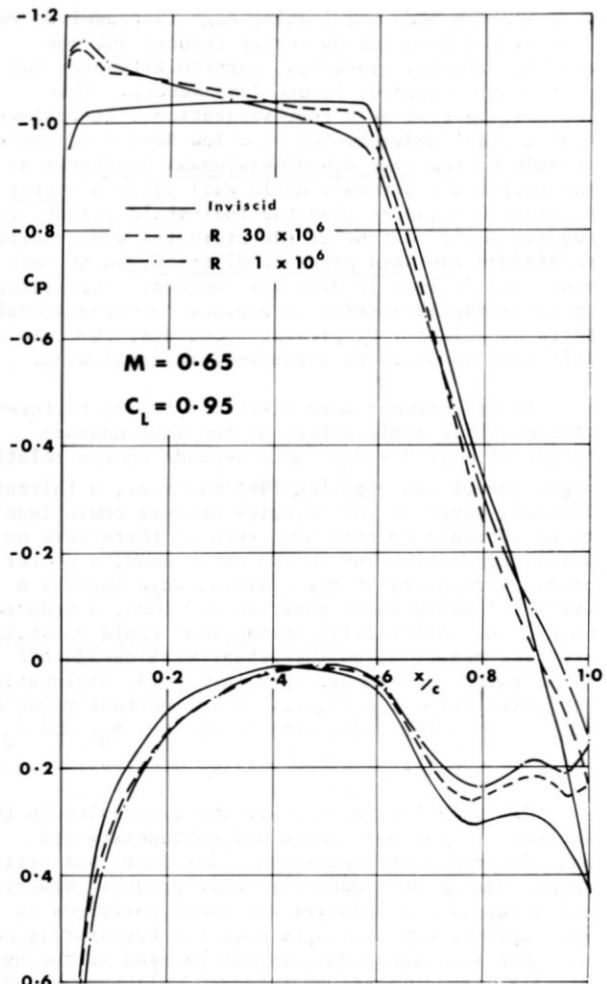
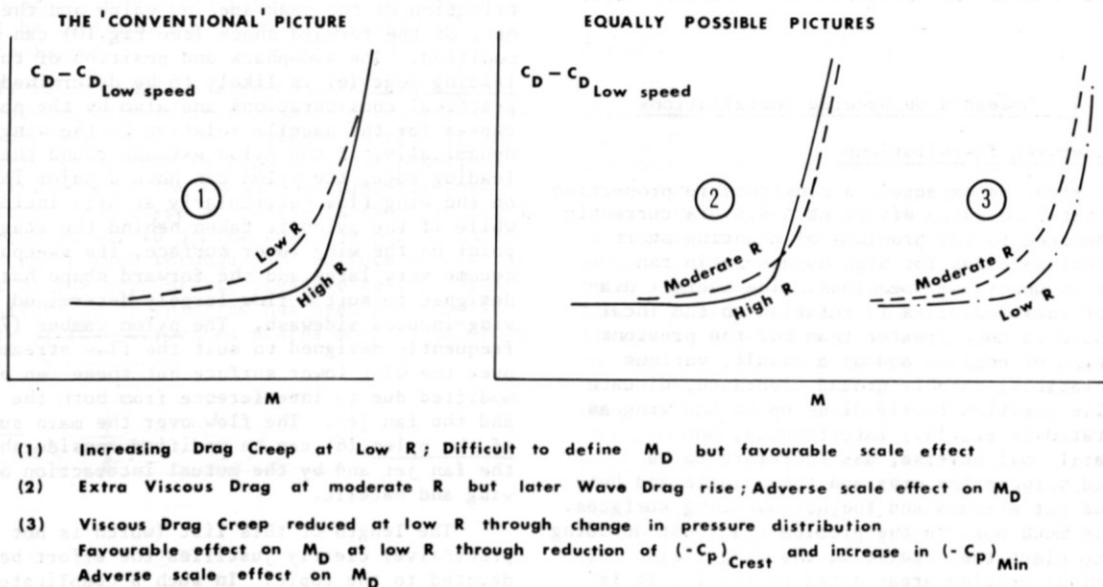


FIG.12 EFFECT OF REYNOLDS NO. ON PRESSURES AT CONSTANT C_L FOR A GIVEN WING SECTION GEOMETRY



- (1) Increasing Drag Creep at Low R; Difficult to define M_D but favourable scale effect
- (2) Extra Viscous Drag at moderate R but later Wave Drag rise; Adverse scale effect on M_D
- (3) Viscous Drag Creep reduced at low R through change in pressure distribution
Favourable effect on M_D at low R through reduction of $(-C_p)_{Crest}$ and increase in $(-C_p)_{Min}$
Adverse scale effect on M_D

FIG.13 POSSIBLE SCALE EFFECTS ON $C_D - M$

peak suction near the leading edge increases therefore as the Reynolds number is reduced but the adverse pressure gradients, particularly over the rear of the surface, become less severe. This lessens the risk of a rear separation. It follows that a small model tested at a low Reynolds number if made to the same non-dimensional ordinates as the full-scale aircraft could well yield a better separation boundary than the full-scale result; the reverse would be true if the ordinates were modified to produce the same pressure distribution at both model and full-scale Reynolds numbers. This second approach has been tried in various two-dimensional tests but clearly on present knowledge, it would be difficult to apply to a three-dimensional wing.

It is somewhat more difficult trying to forecast possible scale effect on the drag characteristics near $M = M_D$. This depends on the relative magnitude of two opposing factors, i.e., a thicker boundary layer at low Reynolds numbers could lead to an increase in form drag even if there were no actual separation but on the other hand, a poorer pressure recovery at the trailing edge implies a further forward shock position and thus, a reduced wave drag. Alternative trends that could exist in practice depending on the actual wing design are illustrated diagrammatically in Fig.13; explanations are given below the figure. The important point to note is that the scale effects on both M_D and C_D at M_D can be either favourable or adverse.

The main lesson from all the discussion in this section is that one should not extrapolate too naively from past experience. The fact that certain techniques in one model test have produced drag-rise and separation boundaries and shock positions in good agreement with flight does not necessarily mean that the same techniques should be used in the next example. Experience and research will provide an intelligent guide to what is required but the proof that the best possible techniques have been used should be sought in a detailed understanding of the flow over the wing design in question - either by means of oil flow studies or wherever possible, measured pressure distributions and boundary layer profiles.

4. Research on Nacelle Installations

4.1 Underwing Installations

As might be expected, a considerable proportion of the total research effort at A.R.A. is currently being devoted to the problems of mounting short front cowl nacelles for high bypass-ratio fan engines in underwing locations. The overall diameter of these nacelles in relation to the local wing chord is much greater than for the previous generation of engines and as a result, various considerations, notably ground clearance, dictate a nacelle position fairly close up to the wing as illustrated in Fig.14. Interference, not necessarily all adverse, has therefore to be accepted between the wing and the nacelle and between the jet streams and the neighbouring surfaces. There is much more to the problem than just deciding where to place the nacelle in the wing field. Of the various problem areas noted in Fig.14, it is probably only item (1), the forward cowl, that can be studied effectively on an isolated nacelle; ideally, all the others should be investigated on a

complete installation with all surfaces and all flows represented. The research at A.R.A. has three main objectives: first, to help in establishing design principles for the various problem area, second, to show what interference drag factors should be feasible and third, to develop techniques for use in routine testing. No results can be presented at this stage but it may be helpful to make some brief comments on various aspects.

Various problem areas are listed in Fig.14. In the past, most forward cowl shapes (1) have been derived from the NACA 1-series. For a given highlight diameter/maximum diameter ratio, if the cowl is too short, the drag-rise Mach number will be too low, while if the cowl is too long, spillage drag or more correctly, excess drag due to flow separation on the cowl will be present up to too high an intake mass-flow ratio. As the highlight diameter ratio is increased, the useable length between these limits contracts until for the values now proposed for the fan cowls, hardly any length is satisfactory from both standpoints. Hence, there is a need for research on improved cowl shapes. As noted earlier, this is the one item on which research can usefully be undertaken on cowls in isolation but even here, there may be scope on an actual installation for yawing, pitching or cambering the cowl in sympathy with the wing flow field. The flow over the aft cowl (2) is affected by forward influence from the fan jet and more particularly, by an adverse pressure gradient imposed by the wing flow field. The "scrubbing drag" (3) on the gas generator is clearly a function of the fan jet velocity but it appears that the pressure distribution on the upper side, i.e., nearer to the wing, can be modified significantly by the influence of the wing and pylon. The wing lower surface (4) is an obvious region for an adverse interference from both the nacelle and the fan jet. This can lead to a reduction in wing C_L at a given incidence and to the premature appearance of a shock wave, particularly inboard of the nacelles if the wing is swept back. The pressure distribution near the leading edge on the wing upper surface (5) can be affected by nacelle-induced upwash and as a result, the spanwise distribution of the peak suction value and the development of the forward shock (see Fig.10) can be modified. The sweepback and position of the pylon leading edge (6) is likely to be determined by practical considerations and also by the position chosen for the nacelle relative to the wing. Aerodynamically, if the pylon extends round the wing leading edge, the pylon can have a major influence on the wing flow particularly at high incidence while if the pylon is taken behind the stagnation point on the wing lower surface, its sweepback can become very large and the forward shape has to be designed to suit a flow largely determined by the wing-induced sidewash. The pylon camber (7) is frequently designed to suit the flow streamline over the wing lower surface but these can be modified due to interference from both the nacelle and the fan jet. The flow over the main surface of the pylon (8) can be modified considerably by the fan jet and by the mutual interaction of the wing and nacelle.

The length of this list (which is not comprehensive) clearly justifies the effort being devoted to the topic! In such a complicated situation, much discussion has tended to arise as to what should be described as "thrust" and what as "drag". A plea must be made at this point that

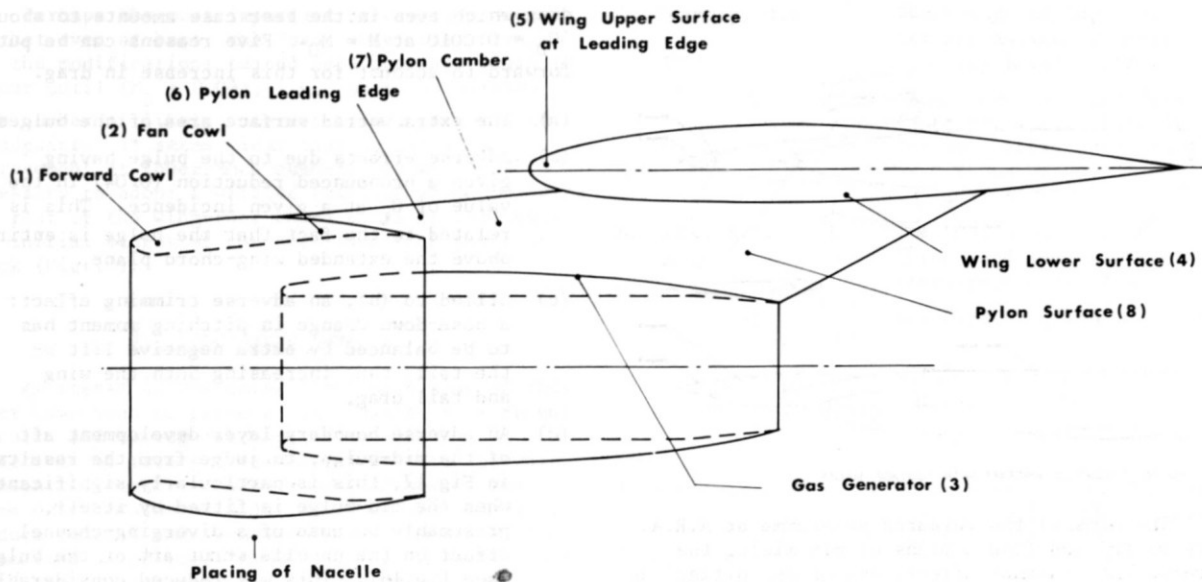


FIG. 14 PROBLEM AREAS FOR WING MOUNTED NACELLE INSTALLATION

the engine and airframe manufacturers must work together and both realise that what really matters is the installed "thrust-minus-drag" due to the addition of a complete engine installation to the rest of the aircraft. If we are to predict, measure and optimise this figure successfully, we must be able to calculate and/or measure the separate contributions for any surfaces where the flow depends significantly on both the aircraft and engine operating conditions and geometry. Any choice of definitions must be somewhat arbitrary; a change in the definitions merely tends to transfer various terms to different parts of the balance sheet, and possibly, to change who is responsible for estimating any particular corrections. What is important are not the particular definitions that may be preferred, but the realisation that anyone who tries to reduce the drag contribution from one particular surface without regard to the remainder may not be contributing to an optimisation of the complete layout!

It is of course easier to make challenging statements on this subject than to put these statements into practice! It is clearly difficult in any single model test to represent all the flows correctly. One of the techniques that has been used with some success at A.R.A. is shown in Fig. 15. High pressure air is ducted down the pylon, taken forward and turned through 180° to form a cold air fan jet at the appropriate pressure ratio. Reasonable uniformity of this jet has been achieved with the help of two perforated plates mounted as shown

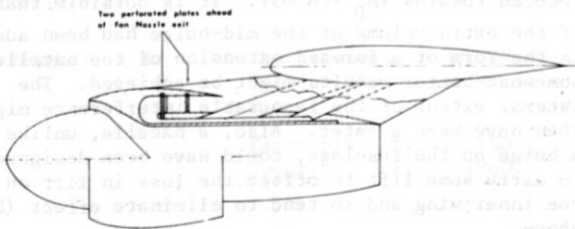


FIG. 15 MODEL NACELLE WITH COLD AIR FAN JET

in the figure. The air for the unboosted gas generator jet is taken in through the intake with the quantity controlled by a large centre-body. Measurements have shown that the use of this centre-body can give pressure distributions over the forward part of the fan cowl representative of the true intake-flow conditions. To date, no overall drag measurements have been made with this technique but extensive pressure plotting has been possible over the fan cowl, gas generator, pylon and wing surfaces. The results have indicated that to optimise a given layout, the fan jet effects (obtained by differencing results for the true fan jet pressure ratio and for an unboosted condition corresponding to a free-flow nacelle) can be quite important and should certainly not be ignored. Other methods for simulating the jet are currently under review.

4.2 Aft-fuselage Installations

The problems of aft-fuselage installations have also been closely investigated in the A.R.A. tunnel during the past few years. The factors that can contribute to the nacelle overall drag increments have been described in Ref. 1. Apart from the profile drag on the nacelle assembly itself, there can be significant contributions from a fore-and-aft redistribution of lift between the wing, tail and nacelles, a spanwise redistribution of lift across the wing, and the effect of the nacelle pressure field on the shock-system over the wing. The degree to which these interference effects are favourable or not depends not merely on the siting of the nacelle assembly but also on the wing aerodynamic characteristics. To take just one illustration, with an arrangement such as that shown in Fig. 16 with the nacelles above the wing plane, there is a reduction in the local lift on the wing ahead of the nacelles. It follows that the incidence for a given C_L on the wing as a whole has to be increased and the interference drag is therefore partly a measure of how the drag of the wing in question reacts to this changed loading.

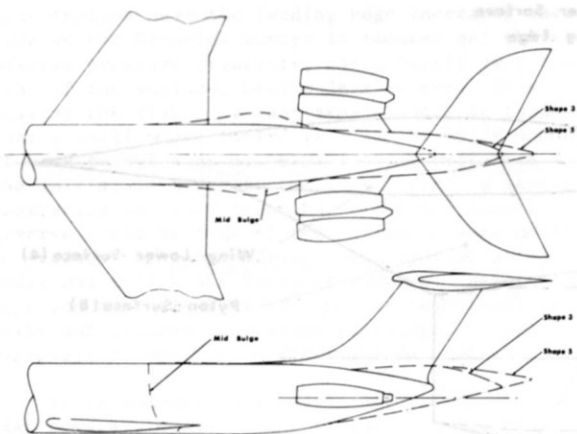


FIG. 16 LAYOUT OF AIRCRAFT WITH FUSELAGE BULGES

The aims of the research programme at A.R.A. were to try and find a means of minimising the adverse interference effects and of exploiting the favourable interference. As with the basic nacelle assembly, many of the results were specific to the installations tested and are therefore difficult to reproduce in a general review paper. However, one set of tests is worthy of special mention particularly since it affords a means of bringing together several points mentioned in the earlier discussion. These tests were made to find the effects of adding some extra "bulges" to the fuselage between the wing and nacelles, and aft of the nacelles. Various alternative shapes were examined, the most successful are those shown in Fig.16. The longitudinal cross-sectional area distribution of the complete aircraft with the bulges fitted gives roughly a uniform value for (dS/dx) from the peak area (S) opposite the wing, back to the tail of the fuselage. In other words, the mid-bulge fills the hole in the area distribution between the wing and the nacelles while the rear bulges fill the hole between the nacelles and tailplane. The measured drag increments due to adding the mid-bulge alone, the mid-bulge in the presence of the rear-bulge, and the rear-bulges are shown in Fig.17. Both trimmed and untrimmed results are included for the mid-bulge; there was no significant effect of trimming for the rear-bulge.

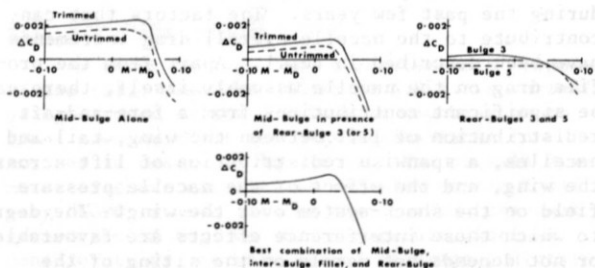


FIG. 17 EFFECT OF FUSELAGE BULGES ON DRAG (see Fig.16)

Considering first the results for the mid-bulge, this clearly begins to have a favourable effect on the shock development over the wing at Mach numbers beyond about $(M_D + 0.03)$ but it does not give a nett drag reduction until beyond $(M_D + 0.05)$. This is because the improvements at high Mach number have to be sufficient to offset a basic increase in

drag which even in the best case amounts to about $\Delta C_D = 0.0010$ at $M = M_D$. Five reasons can be put forward to account for this increase in drag.

- (a) The extra wetted surface area of the bulges,
- (b) Adverse effects due to the bulge having given a pronounced reduction (0.04) in the value of C_L at a given incidence. This is related to the fact that the bulge is entirely above the extended wing-chord plane,
- (c) Allied to (b), an adverse trimming effect: a nose-down change in pitching moment has to be balanced by extra negative lift on the tail, thus increasing both the wing and tail drag,
- (d) An adverse boundary layer development aft of the mid-bulge; to judge from the results in Fig.17, this is particularly significant when the mid-bulge is fitted by itself, presumably because of a diverging-channel effect on the nacelle strut aft of the bulge (see Fig.16). This was reduced considerably when the rear-bulge was also fitted, together with an inter-bulge fillet designed on the basis of oil flow studies. Possibly, the drag increment might have been reduced further by continued development of this fillet,
- (e) Extra nacelle spillage drag. Even if this were true of the model tests, it could clearly be avoided on the aircraft if necessary by a redesign of the nacelle cowl shape.

Not all the factors would apply in every application of this sort of idea. Indeed, only the first is inevitable but this only gives an increment of $0.0002 \Delta C_D$. It follows that further tests might have led to some improvement in the results, but even then, it seems unlikely that any nett drag reduction would have been obtained below $(M_D + 0.03)$ in the present instance.

Turning now to the rear bulges, it appears that these reduce the supercritical drag on some part of the aircraft at Mach numbers above about $(M_D + 0.06)$. At lower Mach numbers, bulge 3 gives a slight increase in drag but bulge 5 gives a nett reduction in drag despite its extra surface area at all Mach numbers. This difference is because the more extended shape 5 is effective in cleaning up a separation near the tip of the bulge on the upper surface.

The overall conclusion is that fitting the best mid- and rear-bulges in combination gives a nett reduction in drag above $(M_D + 0.05)$. With less subcritical drag penalty, this figure could be reduced towards $(M_D + 0.03)$. It is possible that if the extra volume of the mid-bulge had been added in the form of a forward extension of the nacelles, somewhat better results might be achieved. The lateral extent of the favourable interference might then have been greater. Also, a nacelle, unlike a bulge on the fuselage, could have been designed to carry some lift to offset the loss in lift on the inner wing and so tend to eliminate effect (b) above.

Perhaps the most important reservation however is that even at best, the favourable interference for the modifications tested here does not begin to appear until ($M_D + 0.03$), i.e., near the maximum Mach number of likely interest from a performance standpoint. It seems clear that to obtain an improvement at lower Mach numbers, it would be necessary to adopt a waisted fuselage shape opposite the rear of the wing-root chord so as to influence the initial stages of the development of the rear shock (Fig.10).

5. Concluding Remarks

As stated at the outset, the main aims of this paper have been to present some results from recent research and to suggest some of the likely objectives of future research relevant to subsonic transport aircraft. Despite past advances, there seems every reason to hope that this research will produce radical improvements in performance - from a combination of ideas rather than one single source. Three themes have recurred throughout this paper: first, the need to reconcile aerodynamic, structural and other requirements and to establish suitable exchange rates; second, the need for research on how to derive successful configurations with supercritical flow in the design cruise condition as well as an acceptable supercritical development in off-design and third, continued research to ensure that the testing techniques keep pace with the likely changes in wing and nacelle shapes. These must be rated as three of the main objectives for the future.

Finally, the author wishes to acknowledge the help received from other members of the A.R.A. staff and from colleagues in industry and the R.A.E. in the preparation of this paper. He takes full responsibility however for the opinions expressed.

References

1. Haines, A.B. Subsonic Aircraft Drag: An Appreciation of Present Standards
A.R.A. Wind Tunnel Note 66, 1967.
R.Ae.S. Journal pp.253-266, Vol.72, 1968.
2. R.Ae.S. T.D.M.67008
3. R.Ae.S. T.D.M.67009
4. Pearcey, H.H. The Aerodynamic Design of Section Shapes for Swept Wings.
Paper presented at ICAS Congress, Zurich, 1960.
5. Pearcey, H.H. Shock-induced Separation and its Prevention by Design and Boundary Layer Control.
"Boundary Layer and Flow Control", Vol.2, Part IV, Pergamon Press 1961, edited by G.V. Lachmann.
6. Lock, R.C. The Equivalence Law Relating Three- and Two-dimensional Pressure Distributions.
A.R.C.23,952, 1962.
7. R.Ae.S. Data Sheets
Wings 02.04.02
Wings 02.04.03
8. Kuchemann, D. Incompressible Aerodynamics Chapter VIII p.330, 1960, edited by Thwaites.
9. Macdonald, A.G.J. A Note on the Prediction of Aerofoil Profile Drag at Subsonic Speeds.
Nash, J.F.
Osborne, J.
A.R.C.28,075, 1966.
10. Hall, I.M. Experiments with a Tapered Sweptback Wing of Warren 12 Planform at Mach Numbers Between 0.6 and 1.6.
Rogers, E.W.E.
R. & M.3271, 1960.
11. Berry, C.J. A Study of the Effects of Leading-edge Modifications on the Flow over a 55° Sweptback Wing at Transonic Speeds.
Rogers, E.W.E.
Townsend, J.E.G.
A.R.C.21,987, 1960.
12. Haines, A.B. Scale Effects at High Subsonic and Transonic Speeds, and Methods for Fixing Boundary-layer Transition in Model Experiments.
Holder, D.W.
Pearcey, H.H.
R. & M.3012, 1957.
13. Haines, A.B. The Interaction Between Local Effects at the Shock and Rear Separation - a Source of Significant Scale Effects in Wind-tunnel Tests on Aerofoils and Wings.
Pearcey, H.H.
Osborne, J.
Paper to be presented at the AGARD Specialists' Meeting on Transonic Aerodynamics, 18-20 September 1968 - Paris.
14. Powell, B.J. The Calculation of a Pressure Distribution on a Thick Cambered Aerofoil at Subsonic Speeds Including the Effects of Boundary Layer.
A.R.C.29,300, 1967.